HHS Public Access

Author manuscript

Neuropharmacology. Author manuscript; available in PMC 2017 June 01.

Published in final edited form as:

Neuropharmacology. 2016 June ; 105: 84–95. doi:10.1016/j.neuropharm.2016.01.002.

Aβ-mediated spine changes in the hippocampus are microtubule-dependent and can be reversed by a subnanomolar concentration of the microtubule-stabilizing agent epothilone D

Lorène Penazzi[1,*], **Christian Tackenberg**[1,*,#], **Adnan Ghori**[1], **Nataliya Golovyashkina**[1], **Benedikt Niewidok**[1], **Karolin Selle**[1], **Carlo Ballatore**[2,3], **Amos B. Smith III**[2], **Lidia Bakota**[1], and **Roland Brandt**[1]

[1]Department of Neurobiology, University of Osnabrück, Barbarastrasse 11, 49076 Osnabrück, Germany

[2]Department of Chemistry, School of Arts and Sciences, University of Pennsylvania, Philadelphia, Pennsylvania 19104, United States

[3]Center for Neurodegenerative Disease Research, Department of Pathology and Laboratory Medicine, Perelman School of Medicine, University of Pennsylvania, Philadelphia, Pennsylvania 19104, United States

Abstract

Dendritic spines represent the major postsynaptic input of excitatory synapses. Loss of spines and changes in their morphology correlate with cognitive impairment in Alzheimer's disease (AD) and are thought to occur early during pathology. Therapeutic intervention at a preclinical stage of AD to modify spine changes might thus be warranted. To follow the development and to potentially interfere with spine changes over time, we established a long term *ex vivo* model from organotypic cultures of the hippocampus from APP transgenic and control mice. The cultures exhibit spine loss in principal hippocampal neurons, which closely resembles the changes occurring *in vivo*, and spine morphology progressively changes from mushroom-shaped to stubby. We demonstrate that spine changes are completely reversed within few days after blocking amyloid-β (Aβ) production with the gamma-secretase inhibitor DAPT. We show that the microtubule disrupting drug nocodazole leads to spine loss similar to Aβ expressing cultures and suppresses DAPT-mediated spine recovery in slices from APP transgenic mice. Finally, we report that epothilone D (EpoD) at a subnanomolar concentration, which slightly stabilizes microtubules in model neurons, completely reverses Aβ-induced spine loss and increases thin spine density. Taken together the data indicate that Aβ causes spine changes by microtubule destabilization and that spine recovery requires microtubule polymerization. Moreover, our results suggest that a low, subtoxic concentration of EpoD is sufficient to reduce spine loss during the preclinical stage of AD.

[*]Corresponding author: Prof. Dr. Roland Brandt, Department of Neurobiology, University of Osnabrück, Barbarastraße 11, D-49076 Osnabrück, Germany, phone: [+49] (541) 969-2338, FAX: [+49] (541) 969-2354, ; Email: brandt@biologie.uni-osnabrueck.de.
[*]both authors contributed equally
[#]Recent address: Division of Psychiatry Research, University of Zürich, Switzerland.

Conflict of interest: RB owns shares and serves as a scientific advisor for KineMed, Inc., Emeryville, CA. No other potential conflict of interest exists.

INTRODUCTION

Alzheimer's disease (AD) is characterized by massive alterations of the synaptic network as evidenced by loss of postsynaptic spines as well as changes in spine morphology (Baloyannis et al., 2007). Spine loss correlates with cognitive impairment (Scheff et al., 2007), indicating that spine alterations act as a major factor contributing to cognitive dysfunction in AD. Many studies point to a central role of a pathological level of Aβ, probably in the form of soluble dimers or oligomers, that induce synaptic impairment early during the progression of the disease (Lacor et al., 2007; Shankar et al., 2007; Shrestha et al., 2006). In agreement, the presence of Aβ is sufficient to cause synaptic alterations in *ex vivo* cultures and transgenic mice (Jacobsen et al., 2006; Shankar et al., 2008; Tackenberg and Brandt, 2009).

Spines are microcompartments that display critical regulatory roles in the integration of synaptic input and the regulation of synaptic strength (Brandt and Paululat, 2013). According to their shape, spines are generally categorized into three classes, mushroom, stubby and thin (Harris et al., 1992). Mushroom-shaped spines are large, mature spines and may represent "memory spines". In contrast, thin and stubby spines represent immature, more dynamic spines. Thin spines may be "learning spines", and stubby spines could represent general precursors from which thin or mushroom spines protrude (Bourne and Harris, 2007; Petrak et al., 2005). It is also known that changes in spine morphologies are correlated with functional parameters and that the size of the spine neck affects calcium compartimentalization and receptor trafficking (Grunditz et al., 2008; Kusters et al., 2013). Thus spine neck plasticity as it occurs during the transition between mushroom and stubby spines may have a role in changing the processing of local synaptic signals. Loss of mushroom spines is a common feature of several animal and cellular models of AD suggesting that it is a relevant morphological marker for synaptic failure during aging and disease (Tackenberg and Brandt, 2009; Zou et al., 2015) and recently it has been demonstrated that oligomeric Aβ specifically reduces mushroom spines in the hippocampus (Popugaeva et al., 2015).

Spine shape integrity and plasticity heavily depend on actin-cytoskeleton remodelling (Alvarez and Sabatini, 2007). Additionally, more recent studies indicate that microtubules (MTs) transiently invade a subset of mature spines and that changes in MT dynamics affect spine morphing and maintenance (Gu et al., 2008; Hoogenraad and Akhmanova, 2010; Jaworski et al., 2008).

An important question is how changes of spines develop and progress upon chronic exposure to low amounts of Aβ, a likely scenario during the preclinical phase of AD, and how the change in number and the morphology of the spines can be reversed, which in turn might provide an opportunity to interfere with spine changes and the resulting cognitive impairment. In fact, some studies suggest that spines can recover, e.g. by washout acutely added Aβ (Shrestha et al., 2006), or application of neutralizing anti-Aβ antibodies (Spires-Jones et al., 2009). However, whether other treatment options, such as those targeting MT dynamics, could be useful for spine recovery is unknown.

In a previous study we demonstrated that low concentrations of human Aβ lead to a decrease in spine density and a shift in spine morphology from mature to immature spines (Tackenberg and Brandt, 2009). Herein, we have extended the study by establishing a long term *ex vivo* organotypic hippocampal culture to scrutinize the development of spine alterations over time. We further employed this model to analyze the influence of MT-modulating drugs at a time point when spine changes were already evident.

MATERIALS AND METHODS

Animals

Heterozygous APP_{SDL} transgenic C57BL/6 mice (Aventis Pharma, Vitry-sur-Seine, France) and nontransgenic littermates (C57BL/6 mice; Charles River Laboratories, Sulzfeld, Germany and Harlan Winkelmann GmbH, Borchen, Germany) were used. APP_{SDL} transgenic mice express human APP695 with three familial AD mutations under the control of the platelet-derived growth factor β promoter (Blanchard et al., 2003). The mice express human APP at about the same level as murine endogenous APP and produce equal amounts of soluble Aβ 40 and 42 with plaque formation in the hippocampus >18 months of age (Bakota, unpublished observations). All animals were maintained and sacrificed according to National Institutes of Health guidelines and German animal care regulations. Genotyping was performed as described earlier (Tackenberg and Brandt, 2009). For the experiments mice of either gender were used.

Materials

Chemicals were purchased from Sigma (Deisenhofen, Germany). Culture medium and supplements were obtained from Sigma and Invitrogen (Carlsbad, California), culture dishes and plates from Nunc (Roskilde, Denmark) and membrane culture inserts from Millipore (Bedford, MA). Gamma-secretase inhibitor N-[N-(3,5-difluorophenacetyl)-1-alanyl]-S-phenylglycine t-butyl ester (DAPT) was purchased from Merck (Darmstadt, Germany). Epothilone D (EpoD) was prepared as previously described (Lee et al., 2001; Rivkin et al., 2004). The spectroscopic properties of the compound were identical to those reported in the literature. Compound purity was >95% as determined by LC-MS and NMR analyses.

Sindbis virus constructs

Construction of Sindbis virus expressing EGFP-352wt tau was performed as described previously (Shahani et al., 2006; Tackenberg and Brandt, 2009).

Organotypic hippocampal slice cultures and Sindbis virus infection

Organotypic hippocampal slice cultures were prepared and cultured according to (Stoppini et al., 1991). In short, one or two week old APP_{SDL} transgenic or non-transgenic C57BL/6 mice were decapitated, brains were removed, both hippocampi isolated and cut into 400 μm thick slices using McIllwain tissue chopper (Gabler, Bad Schwalbach, Germany). Slices were cultured as described previously (Sundermann et al., 2012; Tackenberg and Brandt, 2009). On day 12 or day 17 *in vitro* slice cultures were infected with Sindbis virus using droplet method (Shahani et al., 2006). For spine analysis, cultures were fixed at day 3 post infection within six-well plates. Slices were left attached to the culture plate membrane to

preserve hippocampal structure and rinsed with PBS. Slices were then fixed with 4% paraformaldehyde in PBS containing 4% sucrose for 2h at 4°C. After washing with PBS, cultures were mounted with Confocal-Matrix (Micro-Tech-Lab, Graz, Austria) and coverslipped.

Treatment of hippocampal slice cultures

To assess potential reversibility of spine changes hippocampal slices were kept for 20 days in culture. Slices were treated with 0.5 μM DAPT, 200 nM nocodazole, or 0.2 nM EpoD from day 16 to day 20. Sindbis virus infection was performed on day 17.

Confocal imaging of fixed hippocampal slices for spine analysis

Confocal high-resolution imaging of spines was performed using Nikon (Tokyo, Japan) confocal laser scanning microscope Eclipse TE2000-U with 60× objective (oil, NA: 1.4) using argon laser (488nm). 20–40 μm long dendritic segments from different hippocampal subregions (secondary and tertiary dendritic segments of *stratum oriens* and *stratum radiatum*) of CA1 and CA3 pyramidal neurons were imaged with voxel size of 0.08 × 0.08 × 0.25 μm in x-y-z direction. Image size was adjusted according to length and shape of the imaged dendritic fragment. Image stacks were further processed as described for morphological spine analysis.

Image processing and semi-automated analysis of spine density and spine morphology

Image stacks (Nikon .ids files) were processed using 3D blind deconvolution (10–15 iterations, Autodeblur software, Watervliet, NY) to improve signal-noise ratio and spatial resolution. Analysis of spine length, volume and shape was performed using 3DMA neuron software (Koh et al., 2002) which allows algorithm-based, semi-automated evaluation of spine morphology in 3D. Spine shape is determined by 3DMA neuron based on the classification of spine shapes (stubby, thin, mushroom), given in (Harris et al., 1992). In general, the decision is based on spine length (L), head diameter (d_h) and neck diameter (d_n) (see Figure 2A, right). For thin spines, spine length is much greater than the neck diameter and head diameter does not exceed neck diameter too excessively. For mushroom spines, length is not excessive, and the head diameter is much greater than the diameter of the neck. For stubby spines, the neck diameter is similar to the length of the spine (the specific criteria are represented in Table 1 of (Koh et al., 2002)). It is possible that due to the deconvolution the spine neck is eliminated from the image. The 3DMA neuron software has clear criteria how to deal with such “detached spine components” and when to include them in the analysis. 3D rendering of dendritic segments and spines for visual representation (see Figure 2 A) was performed on the 3D (deconvolved) image z-stack using the image processing package ImageJ/Fiji (Schindelin et al., 2012). An intensity threshold was set manually to determine the 3D structure of the dendritic segment and the thresholded z-stack was sent for rendering to the 3D Viewer plugin.

Brain fixation and Golgi staining

APP_{SDL} transgenic mice and non-transgenic littermates were immersion fixed (3 week old pups) or perfused transcardially (4 and 5 week old pups) with 4% paraformaldehyde in

phosphate buffer (PFA in PBS), pH 7.4. Brains were stored in PBS at 4°C. For rapid Golgi-staining, brains were stained according to (Hundelt et al., 2011). In short, PFA-fixed brains were incubated in 2.5% (w/v) $K_2Cr_2O_7$ at 34°C for 3 days. The brains were shortly washed in 1% (w/v) $AgNO_3$ and incubated for 4 days at 34°C in 1% (w/v) $AgNO_3$. Coronal sections (200 μm) were cut in 50% (v/v) glycerol with a vibratome and mounted on slides, embedded in Kaiser's glycerol gelatine, and analyzed within two weeks by a blind analysis. Sections were imaged on a Nikon Eclipse TE2000-U fluorescence microscope equipped with a digital camera (Vosskühler COOL-1300). Spine number per μm was determined using the program Lucia G (Nikon).

Photoactivation and live cell imaging of PC12 cells

PC12 cells were cultured, transfected with pIREShyg2-PAGFP-α-tubulin, and neuronally differentiated as described previously (Janning et al., 2014). Cells were pretreated with EpoD or carrier alone (0.01% DMSO) for 30 minutes and imaged within 1 hour on a laser scanning microscope (Eclipse TE2000-U inverted; Nikon) equipped with argon (488 nm) and blue diode (405 nm) lasers. Photoactivation in the middle of a process and automated image acquisition was essentially performed as described previously for 112 seconds at a frequency of 1 frame/s and a resolution of 256×256 pixels (Gauthier-Kemper et al., 2012).

MTT assay

MTT assays were essentially performed as described previously on 96-well plates with a cell number of 10^4 per well (Fath et al., 2002). EpoD or carrier was added 3 hours after plating and MTT conversion was determined after 4 days.

Statistical analysis

Data for dendritic spine analysis are shown as mean ± SEM. The number of mice and dendritic segments, on which analysis for culture experiments was performed, is given in the supplementary tables 1 to 3. Statistical analysis by multiple comparisons between more than two group means employed one-way ANOVA with application of post hoc Tukey's test. Comparison of spine densities of Golgi-stained brains from APP transgenic and non transgenic animals was performed using one way ANOVA with application of post hoc Fisher's LSD test. For all conditions, statistical analysis was based on the number of dendritic segments and was conducted using GraphPad Prism 6.01 software (La Jolla, CA, USA). P values are indicated in the graphs as follows: *(+)(#)<0.05; **(++)(##)<0.01; ***(+++)(###)<0.001. MTT assays were performed in triplicates.

RESULTS

Long term *ex vivo* cultures of APP_{SDL} mice exhibit spine loss over time in CA1 and CA3 hippocampal neurons

We previously demonstrated that cultures from APP_{SDL} transgenic mice produce low equimolar amounts of human $A\beta_{1–42}$ and $A\beta_{1–40}$ already at embryonal age (Leschik et al., 2007). Furthermore we have shown that the presence of Aβ leads to decreased spine density on pyramidal cells of the hippocampus (Tackenberg and Brandt, 2009). To monitor the time sequence of spine changes in an experimentally approachable system, we established a long

term *ex vivo* model in which slices from APP_{SDL} transgenic and control mice were prepared at different days postnatal and cultured for various periods of time to generate cultures of different age (Fig. 1A). We analyzed spines at P7DIV15 as we found dendritic spine pathology evident at this time point in previous studies (Tackenberg and Brandt, 2009). To determine the effect of Aβ on spines over time we further analyzed two different later time points by either increasing the duration in culture (P7DIV20) or by increasing both the duration in culture and the development *in vivo* (P14DIV20). Cultures, which were prepared from 7 or 14 days old mice were vital and could be cultured for up to 20 days and successfully infected using Sindbis virus. We refrained from using older mice or longer culture times since the viability of the cultures decreased and infections were less efficient.

We decided to express EGFP-tagged tau for sensitive visualization of spines by algorithm-based image analysis. The choice was motivated by two reasons: (1) EGFP-tau - compared to EGFP, which shows due to its small size also some nuclear localization - is completely cytosolic and more efficiently labels neurons with all protrusions, (2) we have previously shown that exogenous human tau expression does not interfere with spine density or morphology in hippocampal slices (Shahani et al., 2006; Tackenberg and Brandt, 2009). Furthermore, we and others have shown that transgenic expression of wild type human tau also has no effect on spine density in the hippocampus of mice (Dickstein et al., 2010; Hundelt et al., 2011), although the mice exhibited a shift from mushroom spines to thin spines as a function of human tau aggregation (Dickstein et al., 2010). Very recently it has been confirmed that tau is not required for spine loss in primary neurons (Umeda et al., 2015).

Spine densities were evaluated in dendritic segments from different hippocampal regions to determine potential differences with respect to intrahippocampal connectivity. The method employed confocal high-resolution imaging of fixed slices followed by algorithm-based image analysis with the program 3DMA neuron. We and others had previously shown that this approach allows sensitive and robust evaluation of dendritic spines (Santuccione et al., 2013; Sundermann et al., 2012; Tackenberg et al., 2013). We observed that the density of spines was reduced in most regions and time points in APP_{SDL} transgenic cultures compared to control cultures (Fig. 1B, C). It should be noted that spine density was not affected or even increased in the control slices at the different culture conditions, indicating that our approach permits analyzing spine changes over time at conditions of stable spine populations.

Changes in spine density *ex vivo* resemble the *in vivo* development

Organotypic cultures preserve hippocampal circuitry and recapitulate the *in vivo* development in many aspects (De Simoni et al., 2003). However during longer postnatal periods or increased *in vitro* culture times artefacts may occur. To determine whether the change in spine density *in vivo* reveals a pattern that reflects the early Aβ-related spine loss of the *ex vivo* cultures, brains from APP_{SDL} transgenic mice and control mice were fixed at 3, 4 and 5 weeks of age and stained using a modified Golgi protocol. As shown in Fig. 1A, this age period corresponds to the age of the respective cultures (time of preparation plus days in vitro). Again, dendritic segments of APP_{SDL} transgenic mice had less spines in CA3

st. radiatum compared to control animals (Fig. 1D). Quantification confirmed that the spine density was generally lower at all time points in CA1 and CA3 hippocampal neurons of APP_{SDL} transgenic compared to control mice (Fig. 1E), thus resembling the *ex vivo* data.

Spine shapes progressively change from mushroom to stubby with time of Aβ exposure

Changes in the morphology of spines, which have been associated with functional changes of glutamatergic synapses, may comprise early pathological changes during AD progression (Tackenberg et al., 2009). Spines from APP transgenic cultures showed obvious changes in their morphology compared to control cultures in that they appeared shorter and more stubby-like (Fig. 2A, left). To analyze the morphological changes in a more quantitative manner, we determined the mean spine length at different ages of the cultures. In cultures from APP_{SDL} transgenic mice, spine length was reduced compared to control cultures in several conditions by using multiple comparisons test (Fig. 2B). In most regions the difference in spine lengths markedly increased with the age of the culture. In contrast to the differences in spine lengths, no consistent difference was observed in spine volume, neither with respect to the region nor with respect to the culture time (data not shown). Thus, the data indicate that Aβ induces a progressive shortening of spines while spine volumes remain unaffected.

To scrutinize changes in the shape of spines, the three designating parameters of spine length (L), spine neck (d_n) and head (d_h) diameter were determined for the individual spines, and the spines were then classified into the three categories, “mushroom”, “stubby”, and “thin” by automated image analysis (Figure 2A, right). We found a decreased fraction of mushroom spines in Aβ producing cultures compared to controls, which was most pronounced in older cultures (Fig. 2C). In contrast, the fraction of stubby spines increased in Aβ producing cultures. At the longest culture time (P14DIV20) the population analysis revealed that the decrease in the fraction of mushroom spines and the increase in stubby spines reached significance in all regions by multiple comparisons test (Fig. 2C, bottom row). However, we did not observe a difference in the fraction of thin spines.

Loss of spines and changes in spine morphology are completely reversed after blocking Aβ production with DAPT

Our long term *ex vivo* model provides a system to determine whether, to what extent, and in which time scale Aβ-induced spine changes are reversible. As described before (Tackenberg and Brandt, 2009) and above, changes in spine density and morphology are already present at short culture times in slices from APP_{SDL} transgenic mice compared to control cultures (P7DIV15; Fig. 1C and Fig. 2C) and could be blocked by the presence of the γ-secretase inhibitor DAPT (Tackenberg and Brandt, 2009). Now, to determine how spines respond to a lowering of the amount of Aβ, we added DAPT at a time point when spine changes were already evident (see Fig. 1C) and continued the culture for additional 4 days (P7DIV20; Fig. 3A). Automated spine detection revealed that dendritic segments of DAPT-treated neurons became indistinguishable from untreated control cells (Fig. 3B). Quantification confirmed that DAPT completely abolished the difference in spine densities in the CA1 and the CA3 region between cultures from APP_{SDL} transgenic cultures and control cultures, and that the spine densities in DAPT-treated cultures were similar to untreated controls (Fig, 3C).

Furthermore, DAPT also reversed the shortening of spines, which was most evident in the CA3 region (Fig. 3D). Classification of spine morphologies revealed that DAPT also reversed the shift from mushroom to stubby spines (Fig. 3E). DAPT treatment appeared to cause also a slight increase in mushroom- and a decrease in stubby-shaped spines in control cultures. However, these changes did not reach significance.

Nocodazole induces spine loss of control cultures and suppresses DAPT-induced spine recovery in APP transgenic cultures

Exposure to Aβ is known to induce MT destabilization in cultured neurons (Henriques et al., 2010; Mota et al., 2012) and MTs may be involved in regulating spine morphology and function (Hoogenraad and Akhmanova, 2010; Penazzi et al., 2015). To test for an involvement of MTs we treated the cultures with the MT-disrupting drug nocodazole at a time point when spine changes were already evident (see Fig. 1C), and continued the culture for additional 4 days (P7DIV20, Fig. 4A). Interestingly, we found that while nocodazole caused spine loss in control cultures, this compound did not produce the same effect in Aβ-producing cultures. In fact a small but significant increase in spine density was observed in nocodazole treated APP transgenic cultures (Fig. 4B). Although the small rescuing effect caused by nocodazole in APP transgenic cultures is somewhat surprising, this may result in part from the fact that at low concentrations, MT-depolymerizing agents, including nocodazole, are known to suppress MT dynamic instability (Dent and Kalil, 2001; Mikhailov and Gundersen, 1998). Previously it has been shown that alterations in microtubule dynamics are linked to spine changes (Jaworski et al., 2009). A decrease in the distance and duration of microtubule growth results in a reduced accumulation of scaffolding proteins such as p140Cap in dendritic protrusions, which affects the organization of spine actin as the primary force for spine changes (Hayashi et al., 2011; Repetto et al., 2014). Thus, conditions, which normalize MT dynamics may positively influence actin organization in spines and, at least partially, rescue spine loss. Nocodazole did not affect spine morphology in control cultures as judged from the unchanged fraction of mushroom, stubby and thin spines (Fig. 4C). However it partially reversed the decreased fraction of mushroom spines in APP transgenic cultures, which supports our observation regarding the rescuing effect of nocodazole with respect to the spine density (see Fig. 4B).

To test, whether spine recovery is MT-dependent, we triggered the recovery of the spines by treatment with DAPT either in the absence or in the presence of nocodazole (Fig. 4A). As expected, DAPT treatment alone increased spine density in Aβ-producing cultures, an effect that was suppressed by the simultaneous presence of nocodazole (Fig. 4B). Taken together, the data indicate that Aβ-induced spine loss is indeed mediated by MT disruption and that spine recovery requires MT polymerization.

Subnanomolar concentration of epothilone D reverses spine loss in the presence of Aβ

If MTs are causally involved in spine loss and growth, one might expect that drugs, which modulate MT dynamics, support spine recovery. The epothilones comprise a relatively large class of MT-stabilizing agents (Altmann et al., 2009). Selected brain penetrant examples, such as EpoD, may have neuroprotective activity and have been proposed as potential therapeutic candidates for axonopathies (Barten et al., 2012; Brunden et al., 2010; Lou et al.,

2014; Trushina et al., 2003; Zhang et al., 2012). However dose-dependent neurotoxic effects have also been noted both with certain epothilones as well as other MT-binding agents (Chiorazzi et al., 2009; LaPointe et al., 2013).

Here we wanted to explore, whether low MT-modulating concentrations of EpoD could favorably affect spine parameters in the chronic presence of Aβ. We first determined, in pilot experiments, the effect of EpoD on cell viability using a MTT assay with PC12 cells as a model for rodent neural cells. We observed a major decrease in MTT conversion at a concentration of 50 nM EpoD, while concentrations of 1 nM or below did not cause apparent changes (Fig. 5A). To analyze the effect of EpoD on MT stabilization, we employed a live cell-imaging assay to determine MT dynamics in living neuronal cells. The method is based on determination of fluorescence decay after photoactivation (FDAP) of photoactivatable GFP-tagged (PAGFP-tagged) α-tubulin in a region of a neuronal process (Figure 5B, left). FDAP thus comprises an indicator of the ratio of soluble to polymerized tubulin. EpoD decreased FDAP in a dose dependent manner compared with carrier-treated cells (Fig. 5B, right). Already at a concentration as low as 0.2 nM, EpoD was sufficient to decrease FDAP, indicating MT-stabilizing activity.

To test whether EpoD affects Aβ-induced spine loss, we treated non transgenic and APP transgenic cultures with 0.2 nM EpoD and analyzed spines at P7DIV15 (Fig. 5C, top). We observed that addition of EpoD to slice cultures did not affect spine density in non transgenic cultures but led to a significant increase in spine density in APP transgenic cultures (Fig. 5C, left). It has previously been observed that the presence of taxol detaches tau from microtubules in living cells (Samsonov et al., 2004; Weissmann et al., 2009), which might raise the possibility that the effect of EpoD is influenced by the expression of htau sequence. To test such a scenario, we performed the same experiment also after infection with Sindbis virus expressing EGFP alone, under which conditions we previously observed a similar spine loss due to the presence of Aβ (Tackenberg and Brandt, 2009). We did not see a difference compared to EGFP-tau expressing neurons confirming that the presence of exogenous htau does not affect the loss or gain of spines, also not in the presence of EpoD (Fig. 5C, right). Again, EpoD brought spine density of non transgenic and APP transgenic cultures to the same level. To evaluate a potential effect of EpoD on spine morphology, we determined the fraction of mushroom, stubby and thin spines. Interestingly, EpoD changed the morphology of the spine populations in a way that it increased the fraction of thin spines compared to untreated cultures (Fig. 5D). Such a change was also evident in control cultures.

To determine whether EpoD is also able to reverse Aβ-induced spine loss, we added the compound at 0.2 nM to the slice cultures at a time point when spine changes were already evident (see Fig. 1C) and continued the culture for additional 4 days (Fig. 5E, top). We observed that the density of spines in APP transgenic cultures was much higher compared to untreated controls of the same genotype and reached a level, which was similar to non transgenic controls (Fig. 5F). Also after spine reversal, EpoD changed the morphology of the spine populations in most regions in a way that it increased the fraction of thin spines and decreased the fraction of mushroom spines (Fig. 5H). Again, the respective change was also evident in control cultures suggesting that EpoD induces a shift of the spine population

towards more immature spine types. It is possible that EpoD reinforces synaptogenesis by an increase in the formation of filopodia rather than thin spines. However this is not the case, since the majority of the thin protrusions contained a discernible head indicative of spines (Fig. 5E), and the spine population did not exhibit an increase in spine length (Fig. 5G), which would have been expected after induction of filopodia, which have been reported to be much longer than spines (3–40 μm compared to 0.2–2μm; (Garcia-Lopez et al., 2010)).

DISCUSSION

In this study, we established a long term *ex vivo* model to follow the development of spine changes as they might occur during a presymptomatic stage of AD and proposed a potential therapeutic strategy for their reversal. The major findings are: (1) *ex vivo* cultures exhibit spine changes in CA1 and CA3 hippocampal neurons, which closely resembles the changes occurring *in vivo*; (2) spines completely recover within few days when Aβ is reduced; (3) spine recovery requires MT polymerization and a subnanomolar, non toxic concentration of the MT-stabilizing agent EpoD reverses loss of spines and increases thin spine density.

Loss of dendritic spines and changes in the shape and size of spines are a common abnormality found in human AD brains (Baloyannis et al., 2007). In contrast to the death of neurons, spine loss occurs more widespread (Catala et al., 1988) and appears to be an early event during the development of disease. Indeed, previous studies found that patients in the early stages of AD have much fewer spines in the hippocampus (Scheff et al., 2007). A significant reduction in the number of dendritic spines was also observed in CA1-3 pyramidal neurons in patients with Down's syndrome (DS) before the onset of AD (Ferrer and Gullotta, 1990). This observation is consistent with the hypothesis that spine loss is caused by the increase in the concentration of Aβ due to the gene-doses effect in DS. In our *ex vivo* model, spine loss occurred over time and resembled the *in vivo* results, where it was detectable already at 3 weeks of age. Both, *ex vivo* and *in vivo*, spine loss occurred broadly in different hippocampal subfields, which also resembles the findings in AD patients. It is however noteworthy that spine loss was generally smaller *in vivo* than *ex vivo*, which may indicate that organotypic hippocampal cultures are more sensitive to the presence of Aβ than the hippocampus in intact brains.

Currently, most data suggest that increased levels of Aβ in a soluble, oligomeric form are the major factor that is responsible for the spine changes (Shankar et al., 2007; Tackenberg et al., 2009). This result is also clearly supported by our current data, as we observed that lowering the Aβ load by γ-secretase inhibition not only blocks but completely reverses spine loss and morphological changes with spine morphology being indistinguishable from spine populations that have never been exposed to human Aβ. Furthermore, the data indicate that chronic presence of Aβ causes a gradual change in the morphology of the population of the spines from mushroom to stubby. It should be noted that the age-related morphological changes are in agreement with the hypothesis that mushroom spine loss is a morphological marker for synaptic failure during AD and aging, and stubby spines might be the morphological correlate of the induction of long term depression (Li et al., 2009). However, it needs to be noted that our study focuses on spine changes observed early in development and our long term *ex vivo* culture model might not reproduce all changes, which occur in

older animals in which AD pathology is more established and joined by other pathological hallmarks. Since the preparation of vital organotypic cultures is restricted to young postnatal stages, other approaches would be required. These could involve the use of acute hippocampal slices from animals expressing fluorescent markers in individual neurons, such as the GFP M line (Feng et al., 2000). It will be interesting to determine, whether changes in the population of spines can also be reversed in older animals and whether MT dependent mechanisms are involved.

It has previously been shown that exposure of neuronal cultures to Aβ induces MT destabilization as evidenced by a decreased ratio of acetylated tubulin and reduced MT polymer (Henriques et al., 2010; Mota et al., 2012), however also potential microtubule stabilizing effects have been reported (Pianu et al., 2014) as judged from an increased formation of detyrosinated microtubules. Very recently, Tsushima et al. (Tsushima et al., 2015) provided evidence that Aβ increases MT instability by inhibiting HDAC6, which might provide a direct link between Aβ and the regulation of neuronal microtubule dynamics. This could suggest that the activity of Aβ to induce spine loss is related to its MT destabilizing effect. This is in agreement with our observation that the MT-destabilizing drug nocodazole leads to a loss of spines in control cultures closely resembling the effect of Aβ. It should however be noted that our experiments do not allow to distinguish between a general effect of Aβ on destabilizing pre-existing microtubule networks or interfering with dynamic microtubules that may target spines. The effect of Aβ to induce spine loss in organotypic cultures requires NMDA receptor activation and is independent from the action of tau (Tackenberg and Brandt, 2009; Tackenberg et al., 2013). This differs from reports, where dissociated cultures have been employed and tau-dependent spine loss was observed (Zempel et al., 2013).

Finally, we have demonstrated that a subnanomolar concentration of EpoD at conditions, which slightly stabilize MTs but do not exhibit apparent toxicity, have the potential to completely reverse spine loss even in the continuous presence of Aβ. It should be noted that also low concentrations of nocodazole had a beneficial effect on spine density in slices from APP transgenic mice, whereas nocodazole induced spine loss in non transgenic cultures. Since low concentrations of MT-depolymerizing agents are known to suppress MT dynamic instability (Dent and Kalil, 2001; Mikhailov and Gundersen, 1998), this might point to the fact that physiological spine regulation is dependent on a delicate balance of MT dynamics, where deviations in both directions (increased destabilization on one side or increased stabilization on the other) are of negative impact. We observed that EpoD mediated spine recovery in parallel to the induction of a shift of the spine population towards more immature spine types. Also in control cultures, EpoD led to a similar shift in the population from mushroom to thin spines indicating that even moderate changes in MT dynamics influence spine morphology. This is consistent with previous studies where it has been shown that activity-dependent invasion of MTs in spines alters spine morphology (Hu et al., 2008). The data indicate that MT stabilization by a subnanomolar concentration of EpoD promotes a change in the population of spine types towards more immature spines, which might facilitate spine recovery in a short time interval. It remains however to be shown whether the EpoD-induced increase in spine density is beneficial despite the simultaneous shift of spine morphology. This will require functional analysis, e.g. by electrophysiological

recordings of slice cultures in the presence or absence of EpoD. It should however be noted that behavioural studies provided evidence that treatment with a MT stabilizing drug (paclitaxel) restored memory formation in nocodazole-treated mice (Fanara et al., 2010).

In contrast to paclitaxel and most other taxanes, EpoD and selected congeners are brain penetrant, which is an essential requirement in the development of any CNS active therapeutic candidate for the treatment of AD and related neurodegenerative diseases (Ballatore et al., 2012). Previously it has been reported that EpoD reduces transport deficits and improves cognition in different tau transgenic mice by stabilizing axonal MTs (Barten et al., 2012; Brunden et al., 2010; Zhang et al., 2012), however also a negative impact on dendritic arborisation has been observed (Golovyashkina et al., 2015). Recent data show that EpoB or D promote axon regeneration after transection injury *in vitro* and spinal cord injury (Brizuela et al., 2015; Ruschel et al., 2015). Our data clearly indicate that EpoD, even at very low concentrations, can produce a prominent dendritic effect and rescue spine loss, suggesting that mild modulation of MT dynamics may be an effective strategy to counteract synaptic impairment already in the preclinical state of AD.

Supplementary Material

Refer to Web version on PubMed Central for supplementary material.

Acknowledgments

Funds have been provided by the Deutsche Forschungsgemeinschaft (DFG BR1192/11-2) and the National Institute of Health (U01 AG029213-01A2).

References

Altmann, K.; Hofle, R.; Muller, J.; Mulzer, P. Epothilones: An Outstanding Family of Anti-Tumor Agents: From Soil to The Clinic. Wien, New York: Springer; 2009.

Alvarez VA, Sabatini BL. Anatomical and physiological plasticity of dendritic spines. Annu Rev Neurosci. 2007; 30:79–97. [PubMed: 17280523]

Ballatore C, Brunden KR, Huryn DM, Trojanowski JQ, Lee VM, Smith AB 3rd. Microtubule stabilizing agents as potential treatment for Alzheimer's disease and related neurodegenerative tauopathies. J Med Chem. 2012; 55:8979–8996. [PubMed: 23020671]

Baloyannis SJ, Costa V, Mauroudis I, Psaroulis D, Manolides SL, Manolides LS. Dendritic and spinal pathology in the acoustic cortex in Alzheimer's disease: morphological and morphometric estimation by Golgi technique and electron microscopy. Acta Otolaryngol. 2007; 127:351–354. [PubMed: 17453452]

Barten DM, Fanara P, Andorfer C, Hoque N, Wong PY, Husted KH, Cadelina GW, Decarr LB, Yang L, Liu V, Fessler C, Protassio J, Riff T, Turner H, Janus CG, Sankaranarayanan S, Polson C, Meredith JE, Gray G, Hanna A, et al. Hyperdynamic microtubules, cognitive deficits, and pathology are improved in tau transgenic mice with low doses of the microtubule-stabilizing agent BMS-241027. J Neurosci. 2012; 32:7137–7145. [PubMed: 22623658]

Blanchard V, Moussaoui S, Czech C, Touchet N, Bonici B, Planche M, Canton T, Jedidi I, Gohin M, Wirths O, Bayer TA, Langui D, Duyckaerts C, Tremp G, Pradier L. Time sequence of maturation of dystrophic neurites associated with Abeta deposits in APP/PS1 transgenic mice. Exp Neurol. 2003; 184:247–263. [PubMed: 14637096]

Bourne J, Harris KM. Do thin spines learn to be mushroom spines that remember? Curr Opin Neurobiol. 2007; 17:381–386. [PubMed: 17498943]

Brandt R, Paululat A. Microcompartments in the Drosophila heart and the mammalian brain: general features and common principles. Biol Chem. 2013; 394:217–230. [PubMed: 23314534]

Brizuela M, Blizzard CA, Chuckowree JA, Dawkins E, Gasperini RJ, Young KM, Dickson TC. The microtubule-stabilizing drug Epothilone D increases axonal sprouting following transection injury in vitro. Mol Cell Neurosci. 2015; 66:129–140. [PubMed: 25684676]

Brunden KR, Zhang B, Carroll J, Yao Y, Potuzak JS, Hogan AM, Iba M, James MJ, Xie SX, Ballatore C, Smith AB 3rd, Lee VM, Trojanowski JQ. Epothilone D improves microtubule density, axonal integrity, and cognition in a transgenic mouse model of tauopathy. J Neurosci. 2010; 30:13861–13866. [PubMed: 20943926]

Catala I, Ferrer I, Galofre E, Fabregues I. Decreased numbers of dendritic spines on cortical pyramidal neurons in dementia. A quantitative Golgi study on biopsy samples. Hum Neurobiol. 1988; 6:255–259. [PubMed: 3350705]

Chiorazzi A, Nicolini G, Canta A, Oggioni N, Rigolio R, Cossa G, Lombardi R, Roglio I, Cervellini I, Lauria G, Melcangi RC, Bianchi R, Crippa D, Cavaletti G. Experimental epothilone B neurotoxicity: results of in vitro and in vivo studies. Neurobiol Dis. 2009; 35:270–277. [PubMed: 19464369]

De Simoni A, Griesinger CB, Edwards FA. Development of rat CA1 neurones in acute versus organotypic slices: role of experience in synaptic morphology and activity. J Physiol. 2003; 550:135–147. [PubMed: 12879864]

Dent EW, Kalil K. Axon branching requires interactions between dynamic microtubules and actin filaments. J Neurosci. 2001; 21:9757–9769. [PubMed: 11739584]

Dickstein DL, Brautigam H, Stockton SD Jr, Schmeidler J, Hof PR. Changes in dendritic complexity and spine morphology in transgenic mice expressing human wild-type tau. Brain Struct Funct. 2010; 214:161–179. [PubMed: 20213269]

Fanara P, Husted KH, Selle K, Wong PY, Banerjee J, Brandt R, Hellerstein MK. Changes in microtubule turnover accompany synaptic plasticity and memory formation in response to contextual fear conditioning in mice. Neuroscience. 2010; 168:167–178. [PubMed: 20332016]

Fath T, Eidenmuller J, Brandt R. Tau-mediated cytotoxicity in a pseudohyperphosphorylation model of Alzheimer's disease. J Neurosci. 2002; 22:9733–9741. [PubMed: 12427828]

Feng G, Mellor RH, Bernstein M, Keller-Peck C, Nguyen QT, Wallace M, Nerbonne JM, Lichtman JW, Sanes JR. Imaging neuronal subsets in transgenic mice expressing multiple spectral variants of GFP. Neuron. 2000; 28:41–51. [PubMed: 11086982]

Ferrer I, Gullotta F. Down's syndrome and Alzheimer's disease: dendritic spine counts in the hippocampus. Acta Neuropathol. 1990; 79:680–685. [PubMed: 2141748]

Garcia-Lopez P, Garcia-Marin V, Freire M. Dendritic spines and development: towards a unifying model of spinogenesis--a present day review of Cajal's histological slides and drawings. Neural Plast. 2010; 2010:769207. [PubMed: 21584262]

Gauthier-Kemper A, Weissmann C, Reyher HJ, Brandt R. Monitoring cytoskeletal dynamics in living neurons using fluorescence photoactivation. Methods Enzymol. 2012; 505:3–21. [PubMed: 22289445]

Golovyashkina N, Penazzi L, Ballatore C, Smith A III, Bakota L, Brandt R. Region-specific dendritic simplification induced by Abeta, mediated by tau via dysregulation of microtubule dynamics: a mechanistic distinct event from other neurodegenerative processes. Mol Neurodegen. 2015; doi: 10.1186/s13024-13015-10049-13020

Grunditz A, Holbro N, Tian L, Zuo Y, Oertner TG. Spine neck plasticity controls postsynaptic calcium signals through electrical compartmentalization. J Neurosci. 2008; 28:13457–13466. [PubMed: 19074019]

Gu J, Firestein BL, Zheng JQ. Microtubules in dendritic spine development. J Neurosci. 2008; 28:12120–12124. [PubMed: 19005076]

Harris KM, Jensen FE, Tsao B. Three-dimensional structure of dendritic spines and synapses in rat hippocampus (CA1) at postnatal day 15 and adult ages: implications for the maturation of synaptic physiology and long-term potentiation. J Neurosci. 1992; 12:2685–2705. [PubMed: 1613552]

Hayashi K, Suzuki A, Hirai S, Kurihara Y, Hoogenraad CC, Ohno S. Maintenance of dendritic spine morphology by partitioning-defective 1b through regulation of microtubule growth. J Neurosci. 2011; 31:12094–12103. [PubMed: 21865452]

Henriques AG, Vieira SI, da Cruz ESEF, da Cruz ESOA. Abeta promotes Alzheimer's disease-like cytoskeleton abnormalities with consequences to APP processing in neurons. J Neurochem. 2010; 113:761–771. [PubMed: 20345756]

Hoogenraad CC, Akhmanova A. Dendritic spine plasticity: new regulatory roles of dynamic microtubules. Neuroscientist. 2010; 16:650–661. [PubMed: 21239729]

Hu X, Viesselmann C, Nam S, Merriam E, Dent EW. Activity-dependent dynamic microtubule invasion of dendritic spines. J Neurosci. 2008; 28:13094–13105. [PubMed: 19052200]

Hundelt M, Fath T, Selle K, Oesterwind K, Jordan J, Schultz C, Gotz J, von Engelhardt J, Monyer H, Lewejohann L, Sachser N, Bakota L, Brandt R. Altered phosphorylation but no neurodegeneration in a mouse model of tau hyperphosphorylation. Neurobiol Aging. 2011; 32:991–1006. [PubMed: 19660835]

Jacobsen JS, Wu CC, Redwine JM, Comery TA, Arias R, Bowlby M, Martone R, Morrison JH, Pangalos MN, Reinhart PH, Bloom FE. Early-onset behavioral and synaptic deficits in a mouse model of Alzheimer's disease. Proc Natl Acad Sci U S A. 2006; 103:5161–5166. [PubMed: 16549764]

Janning D, Igaev M, Sundermann F, Bruhmann J, Beutel O, Heinisch JJ, Bakota L, Piehler J, Junge W, Brandt R. Single-molecule tracking of tau reveals fast kiss-and-hop interaction with microtubules in living neurons. Mol Biol Cell. 2014; 25:3541–3551. [PubMed: 25165145]

Jaworski J, Hoogenraad CC, Akhmanova A. Microtubule plus-end tracking proteins in differentiated mammalian cells. Int J Biochem Cell Biol. 2008; 40:619–637. [PubMed: 18023603]

Jaworski J, Kapitein LC, Gouveia SM, Dortland BR, Wulf PS, Grigoriev I, Camera P, Spangler SA, Di Stefano P, Demmers J, Krugers H, Defilippi P, Akhmanova A, Hoogenraad CC. Dynamic microtubules regulate dendritic spine morphology and synaptic plasticity. Neuron. 2009; 61:85–100. [PubMed: 19146815]

Koh IY, Lindquist WB, Zito K, Nimchinsky EA, Svoboda K. An image analysis algorithm for dendritic spines. Neural Comput. 2002; 14:1283–1310. [PubMed: 12020447]

Kusters R, Kapitein LC, Hoogenraad CC, Storm C. Shape-induced asymmetric diffusion in dendritic spines allows efficient synaptic AMPA receptor trapping. Biophys J. 2013; 105:2743–2750. [PubMed: 24359746]

Lacor PN, Buniel MC, Furlow PW, Clemente AS, Velasco PT, Wood M, Viola KL, Klein WL. Abeta oligomer-induced aberrations in synapse composition, shape, and density provide a molecular basis for loss of connectivity in Alzheimer's disease. J Neurosci. 2007; 27:796–807. [PubMed: 17251419]

LaPointe NE, Morfini G, Brady ST, Feinstein SC, Wilson L, Jordan MA. Effects of eribulin, vincristine, paclitaxel and ixabepilone on fast axonal transport and kinesin-1 driven microtubule gliding: implications for chemotherapy-induced peripheral neuropathy. Neurotoxicology. 2013; 37:231–239. [PubMed: 23711742]

Lee CB, Wu Z, Zhang F, Chappell MD, Stachel SJ, Chou TC, Guan Y, Danishefsky SJ. Insights into long-range structural effects on the stereochemistry of aldol condensations: a practical total synthesis of desoxyepothilone F. J Am Chem Soc. 2001; 123:5249–5259. [PubMed: 11457387]

Leschik J, Welzel A, Weissmann C, Eckert A, Brandt R. Inverse and distinct modulation of tau-dependent neurodegeneration by presenilin 1 and amyloid-beta in cultured cortical neurons: evidence that tau phosphorylation is the limiting factor in amyloid-beta-induced cell death. J Neurochem. 2007; 101:1303–1315. [PubMed: 17298384]

Li S, Hong S, Shepardson NE, Walsh DM, Shankar GM, Selkoe D. Soluble oligomers of amyloid Beta protein facilitate hippocampal long-term depression by disrupting neuronal glutamate uptake. Neuron. 2009; 62:788–801. [PubMed: 19555648]

Lou K, Yao Y, Hoye AT, James MJ, Cornec AS, Hyde E, Gay B, Lee VM, Trojanowski JQ, Smith AB 3rd, Brunden KR, Ballatore C. Brain-penetrant, orally bioavailable microtubule-stabilizing small molecules are potential candidate therapeutics for Alzheimer's disease and related tauopathies. J Med Chem. 2014; 57:6116–6127. [PubMed: 24992153]

Mikhailov A, Gundersen GG. Relationship between microtubule dynamics and lamellipodium formation revealed by direct imaging of microtubules in cells treated with nocodazole or taxol. Cell Motil Cytoskeleton. 1998; 41:325–340. [PubMed: 9858157]

Mota SI, Ferreira IL, Pereira C, Oliveira CR, Rego AC. Amyloid-beta peptide 1–42 causes microtubule deregulation through N-methyl-D-aspartate receptors in mature hippocampal cultures. Curr Alzheimer Res. 2012; 9:844–856. [PubMed: 22631440]

Penazzi L, Bakota L, Brandt R. Microtubule dynamics in neuronal development, plasticity and neurodegeneration. Int Rev Cell Mol Biol. 2015 in press.

Petrak LJ, Harris KM, Kirov SA. Synaptogenesis on mature hippocampal dendrites occurs via filopodia and immature spines during blocked synaptic transmission. J Comp Neurol. 2005; 484:183–190. [PubMed: 15736233]

Pianu B, Lefort R, Thuiliere L, Tabourier E, Bartolini F. The Abeta(1)(−)(4)(2) peptide regulates microtubule stability independently of tau. J Cell Sci. 2014; 127:1117–1127. [PubMed: 24424028]

Popugaeva E, Pchitskaya E, Speshilova A, Alexandrov S, Zhang H, Vlasova O, Bezprozvanny I. STIM2 protects hippocampal mushroom spines from amyloid synaptotoxicity. Mol Neurodegener. 2015; 10:37. [PubMed: 26275606]

Repetto D, Camera P, Melani R, Morello N, Russo I, Calcagno E, Tomasoni R, Bianchi F, Berto G, Giustetto M, Berardi N, Pizzorusso T, Matteoli M, Di Stefano P, Missler M, Turco E, Di Cunto F, Defilippi P. p140Cap regulates memory and synaptic plasticity through Src-mediated and citron-N-mediated actin reorganization. J Neurosci. 2014; 34:1542–1553. [PubMed: 24453341]

Rivkin A, Yoshimura F, Gabarda AE, Cho YS, Chou TC, Dong H, Danishefsky SJ. Discovery of (E)-9,10-dehydroepothilones through chemical synthesis: on the emergence of 26-trifluoro-(E)-9,10-dehydro-12,13-desoxyepothilone B as a promising anticancer drug candidate. J Am Chem Soc. 2004; 126:10913–10922. [PubMed: 15339176]

Ruschel J, Hellal F, Flynn KC, Dupraz S, Elliott DA, Tedeschi A, Bates M, Sliwinski C, Brook G, Dobrindt K, Peitz M, Brustle O, Norenberg MD, Blesch A, Weidner N, Bunge MB, Bixby JL, Bradke F. Axonal regeneration. Systemic administration of epothilone B promotes axon regeneration after spinal cord injury. Science. 2015; 348:347–352. [PubMed: 25765066]

Samsonov A, Yu JZ, Rasenick M, Popov SV. Tau interaction with microtubules in vivo. J Cell Sci. 2004; 117:6129–6141. [PubMed: 15564376]

Santuccione AC, Merlini M, Shetty A, Tackenberg C, Bali J, Ferretti MT, McAfoose J, Kulic L, Bernreuther C, Welt T, Grimm J, Glatzel M, Rajendran L, Hock C, Nitsch RM. Active vaccination with ankyrin G reduces beta-amyloid pathology in APP transgenic mice. Mol Psychiatry. 2013; 18:358–368. [PubMed: 22688190]

Scheff SW, Price DA, Schmitt FA, DeKosky ST, Mufson EJ. Synaptic alterations in CA1 in mild Alzheimer disease and mild cognitive impairment. Neurology. 2007; 68:1501–1508. [PubMed: 17470753]

Schindelin J, Arganda-Carreras I, Frise E, Kaynig V, Longair M, Pietzsch T, Preibisch S, Rueden C, Saalfeld S, Schmid B, Tinevez JY, White DJ, Hartenstein V, Eliceiri K, Tomancak P, Cardona A. Fiji: an open-source platform for biological-image analysis. Nat Methods. 2012; 9:676–682. [PubMed: 22743772]

Shahani N, Subramaniam S, Wolf T, Tackenberg C, Brandt R. Tau aggregation and progressive neuronal degeneration in the absence of changes in spine density and morphology after targeted expression of Alzheimer's disease-relevant tau constructs in organotypic hippocampal slices. J Neurosci. 2006; 26:6103–6114. [PubMed: 16738255]

Shankar GM, Bloodgood BL, Townsend M, Walsh DM, Selkoe DJ, Sabatini BL. Natural oligomers of the Alzheimer amyloid-beta protein induce reversible synapse loss by modulating an NMDA-type glutamate receptor-dependent signaling pathway. J Neurosci. 2007; 27:2866–2875. [PubMed: 17360908]

Shankar GM, Li S, Mehta TH, Garcia-Munoz A, Shepardson NE, Smith I, Brett FM, Farrell MA, Rowan MJ, Lemere CA, Regan CM, Walsh DM, Sabatini BL, Selkoe DJ. Amyloid-beta protein dimers isolated directly from Alzheimer's brains impair synaptic plasticity and memory. Nat Med. 2008; 14:837–842. [PubMed: 18568035]

Shrestha BR, Vitolo OV, Joshi P, Lordkipanidze T, Shelanski M, Dunaevsky A. Amyloid beta peptide adversely affects spine number and motility in hippocampal neurons. Mol Cell Neurosci. 2006; 33:274–282. [PubMed: 16962789]

Spires-Jones TL, Mielke ML, Rozkalne A, Meyer-Luehmann M, de Calignon A, Bacskai BJ, Schenk D, Hyman BT. Passive immunotherapy rapidly increases structural plasticity in a mouse model of Alzheimer disease. Neurobiol Dis. 2009; 33:213–220. [PubMed: 19028582]

Stoppini L, Buchs PA, Muller D. A simple method for organotypic cultures of nervous tissue. J Neurosci Methods. 1991; 37:173–182. [PubMed: 1715499]

Sundermann F, Golovyashkina N, Tackenberg C, Brandt R, Bakota L. High-resolution imaging and evaluation of spines in organotypic hippocampal slice cultures. Methods Mol Biol. 2012; 846:277–293. [PubMed: 22367819]

Tackenberg C, Brandt R. Divergent pathways mediate spine alterations and cell death induced by amyloid-beta, wild-type tau, and R406W tau. J Neurosci. 2009; 29:14439–14450. [PubMed: 19923278]

Tackenberg C, Ghori A, Brandt R. Thin, stubby or mushroom: spine pathology in Alzheimer's disease. Curr Alzheimer Res. 2009; 6:261–268. [PubMed: 19519307]

Tackenberg C, Grinschgl S, Trutzel A, Santuccione AC, Frey MC, Konietzko U, Grimm J, Brandt R, Nitsch RM. NMDA receptor subunit composition determines beta-amyloid-induced neurodegeneration and synaptic loss. Cell Death Dis. 2013; 4:e608. [PubMed: 23618906]

Trushina E, Heldebrant MP, Perez-Terzic CM, Bortolon R, Kovtun IV, Badger JD 2nd, Terzic A, Estevez A, Windebank AJ, Dyer RB, Yao J, McMurray CT. Microtubule destabilization and nuclear entry are sequential steps leading to toxicity in Huntington's disease. Proc Natl Acad Sci U S A. 2003; 100:12171–12176. [PubMed: 14527999]

Tsushima H, Emanuele M, Polenghi A, Esposito A, Vassalli M, Barberis A, Difato F, Chieregatti E. HDAC6 and RhoA are novel players in Abeta-driven disruption of neuronal polarity. Nat Commun. 2015; 6:7781. [PubMed: 26198811]

Umeda T, Ramser EM, Yamashita M, Nakajima K, Mori H, Silverman MA, Tomiyama T. Intracellular amyloid beta oligomers impair organelle transport and induce dendritic spine loss in primary neurons. Acta Neuropathol Commun. 2015; 3:51. [PubMed: 26293809]

Weissmann C, Reyher HJ, Gauthier A, Steinhoff HJ, Junge W, Brandt R. Microtubule binding and trapping at the tip of neurites regulate tau motion in living neurons. Traffic. 2009; 10:1655–1668. [PubMed: 19744140]

Zempel H, Luedtke J, Kumar Y, Biernat J, Dawson H, Mandelkow E, Mandelkow EM. Amyloid-beta oligomers induce synaptic damage via Tau-dependent microtubule severing by TTLL6 and spastin. EMBO J. 2013; 32:2920–2937. [PubMed: 24065130]

Zhang B, Carroll J, Trojanowski JQ, Yao Y, Iba M, Potuzak JS, Hogan AM, Xie SX, Ballatore C, Smith AB 3rd, Lee VM, Brunden KR. The microtubule-stabilizing agent, epothilone D, reduces axonal dysfunction, neurotoxicity, cognitive deficits, and Alzheimer-like pathology in an interventional study with aged tau transgenic mice. J Neurosci. 2012; 32:3601–3611. [PubMed: 22423084]

Zou C, Montagna E, Shi Y, Peters F, Blazquez-Llorca L, Shi S, Filser S, Dorostkar MM, Herms J. Intraneuronal APP and extracellular Abeta independently cause dendritic spine pathology in transgenic mouse models of Alzheimer's disease. Acta Neuropathol. 2015; 129:909–920. [PubMed: 25862638]

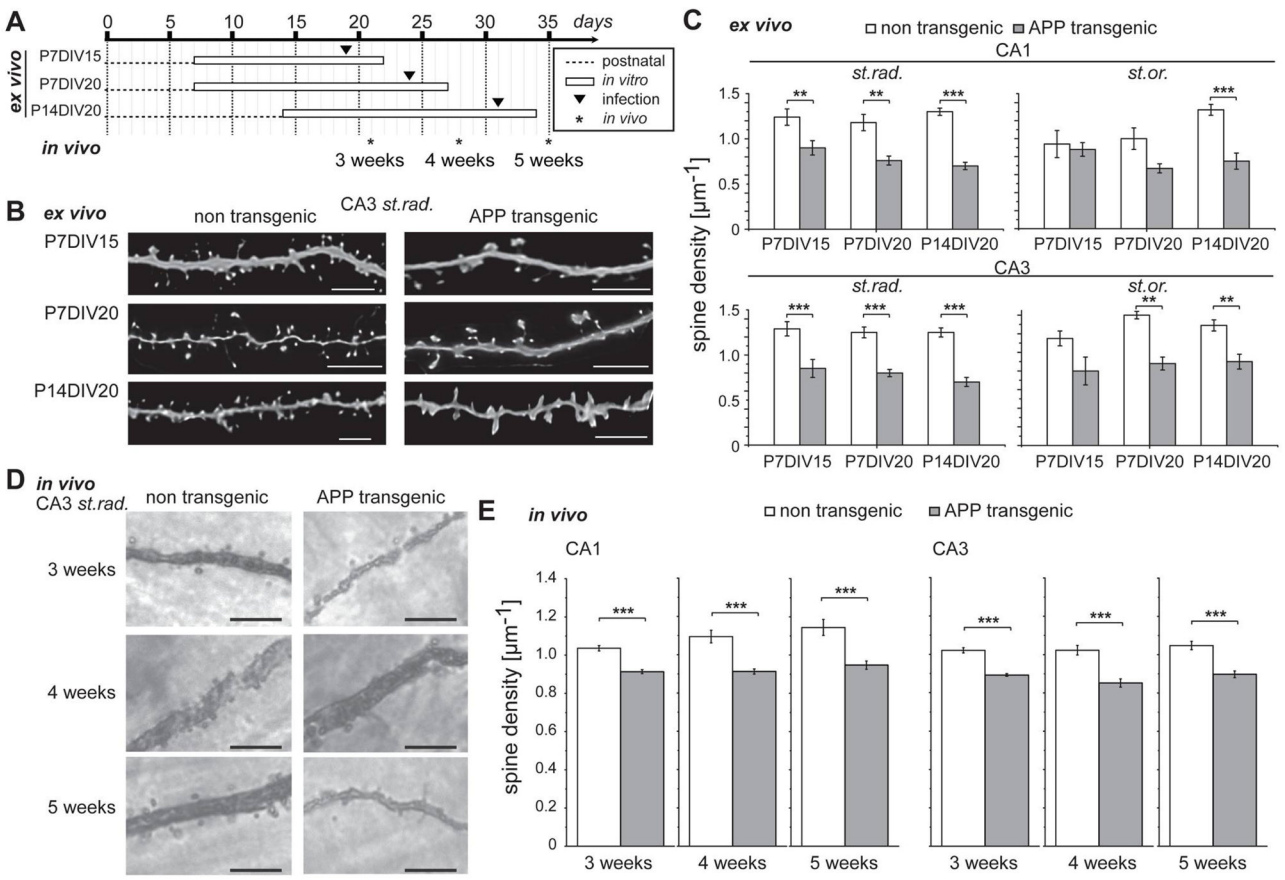

Figure 1. Spine loss *in vivo* and in an *ex vivo* model of Alzheimer's disease

A. Schematic representation showing the conditions to analyze the development of spine changes at different ages. Hippocampal slices were prepared from 7 or 14 days old mice and kept in culture for 15 or 20 days. All slices were infected 3 days before analysis with EGFP-tagged tau for spine visualization. Time points when spine densities were determined *in vivo* are indicated by asterisks at the bottom. **B**. Representative high-resolution images of dendritic segments of CA3 neurons (*st.rad.*) at the conditions shown in (A). **C**. Effect of culture time on spine densities in APP_{SDL} transgenic and non-transgenic cultures (CA1 and CA3 neurons; *st.rad., st.or.*). Spine density is reduced in cultures from APP_{SDL} transgenic mice compared to non-transgenic controls. **D.** Representative images of dendritic segments of CA3 neurons (*st.rad.*) from Golgi-stained brains from 3–5 week old APP_{SDL} transgenic and non-transgenic mice. **E.** Effect of age on spine densities in APP_{SDL} transgenic and non-transgenic animals (CA1 and CA3 neurons). Spine density is reduced in brains from APP_{SDL} transgenic mice compared to non-transgenic controls.

Images in (B) were processed by blind deconvolution with Autodeblur software. Values are shown as mean ± SEM. Statistical evaluation was performed using one way ANOVA with application of post hoc Tukey's test for multiple comparisons (C) or post hoc Fisher's LSD test (E). See supplementary table 1 for details on the statistics of the culture experiments. Values in (E) are shown as mean ± SEM (n=10–12 (CA1), n=10–11 (CA3) from at least

three mice per condition). **p<0.01, ***p<0.001. Scale bar, 5μm (B, D). *st.or.*, *stratum oriens; st.rad.*, *stratum radiatum*; P, days post natal; DIV, days *in vitro*.

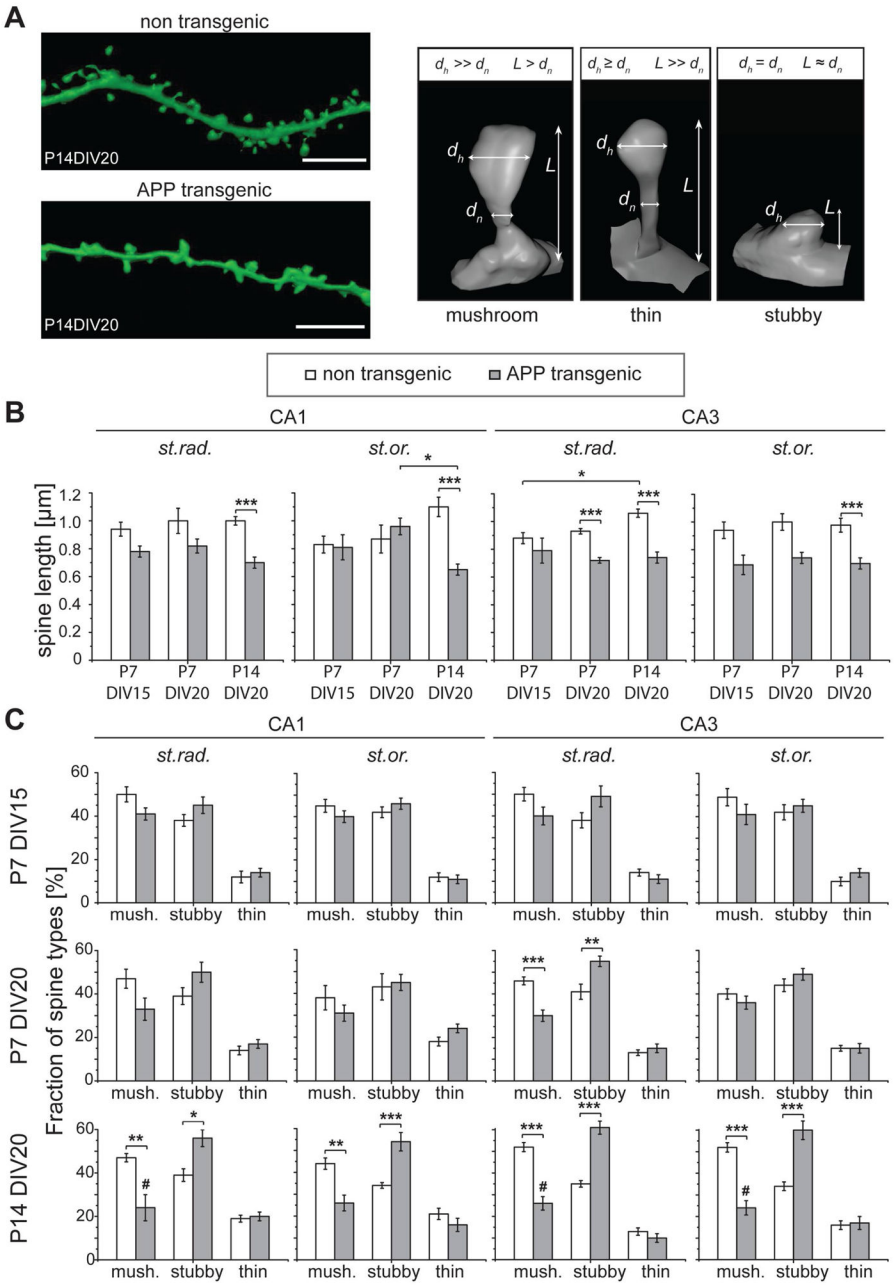

Figure 2. Change of spine shapes during *ex vivo* culture

A. Representative high resolution images of dendritic segments from CA3 st.rad. from P14DIV20 APP_{SDL} transgenic and non-transgenic cultures after 3D rendering. The three spine categories and the designating parameters spine length (L), spine neck (d_n) and head (d_h) diameter are shown at the right. **B.** Effect of age on spine lengths in APP_{SDL} transgenic and non-transgenic cultures (CA1 and CA3 neurons; st.rad., st.or.). Spine length is significantly reduced at several conditions in cultures from APP_{SDL} transgenic mice compared to non-transgenic controls as analyzed by Tukey's multiple comparisons test. **C**. Effect of age on spine shape. The fraction of mature, mushroom-shaped spines decreases

whereas immature, stubby spines increase in cultures from APP_{SDL} transgenic mice compared to non-transgenic controls. The shift from mushroom to stubby spines is most evident in the oldest cultures (P14DIV20).

3D rendering of dendritic segments and spines for visual representation in (A) was performed on the 3D (deconvolved) image z-stack using ImageJ/Fiji as described in "Materials and Methods". (#) indicate significant decrease compared to the respective genotype at P7DIV15. All values are shown as mean ± SEM. Statistical evaluation was performed using one way ANOVA with application of post hoc Tukey's test for multiple comparisons. See supplementary tables 2 and 3 for details on the statistics. *st.or.*, *stratum oriens; st.rad.*, *stratum radiatum*; P, days post natal; DIV, days *in vitro;* mush., mushroom-shaped spine. *(#)$p<0.05$, **$p<0.01$, ***$p<0.001$. Scale bar: 5μm.

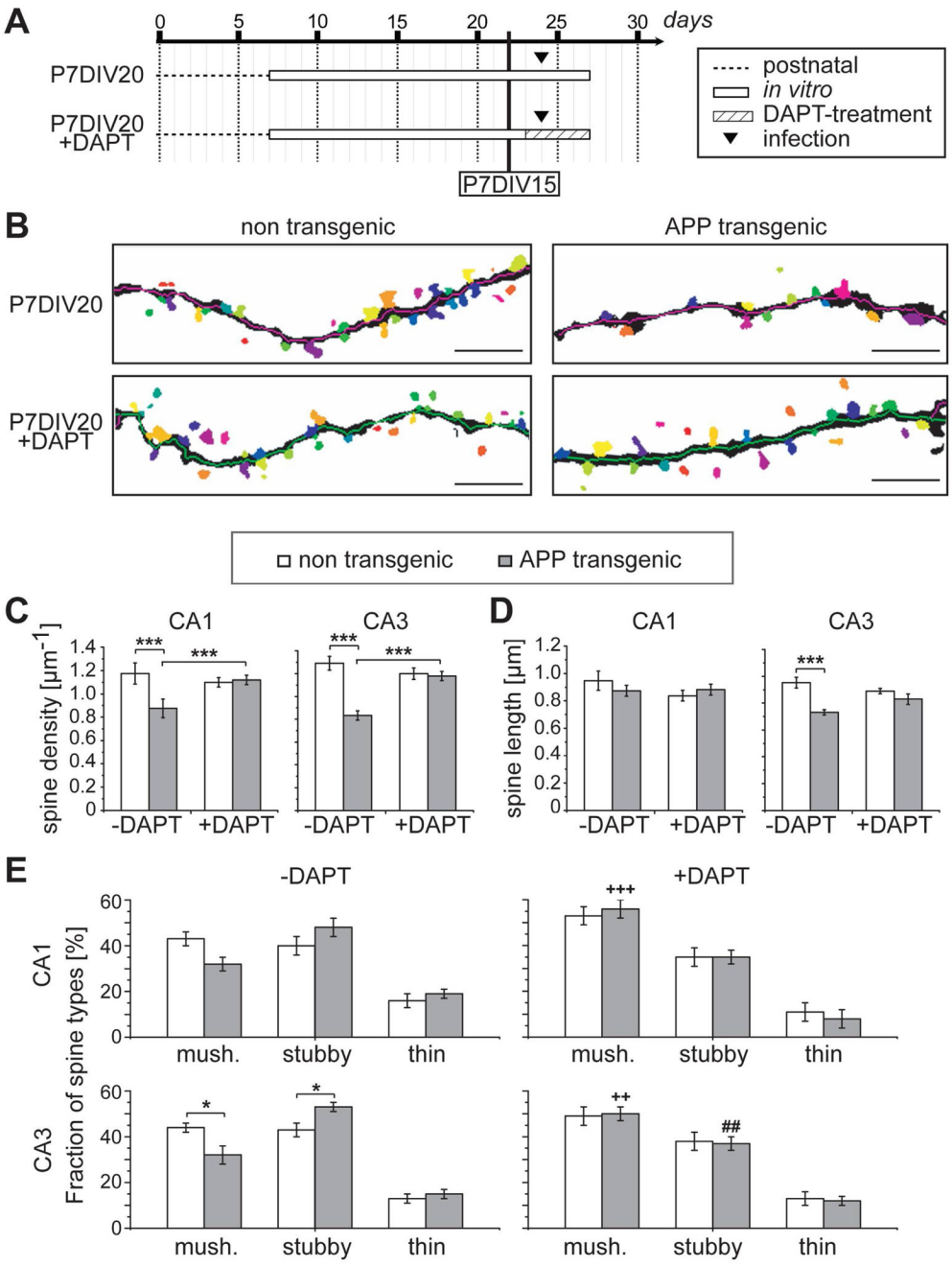

Figure 3. Reversal of spine changes by DAPT

A. Schematic representation showing the experimental set-up to analyze the recovery of spines. Hippocampal slices were prepared from 7 days old mice and kept in culture for 20 days. Aβ-production was blocked from day 16 by adding the γ-secretase inhibitor DAPT. Conditions, where spine changes were already evident in cultures from APP_{SDL} transgenic mice (P7DIV15), are indicated. **B.** Representative images of dendritic segments of CA3 neurons from non-transgenic and APP_{SDL} transgenic cultures treated with or without DAPT for 4 days. Individual spines were detected using 3DMA neuron software. **C–E.** Effect of DAPT-treatment on spine densities (C), spine lengths (D), and spine shape (E) in CA1 and

CA3 neurons. Differences compared to the respective genotype without the drug are indicated. After DAPT treatment, spine density, spine length and spine shape from APP_{SDL} transgenic mice are reversed to control conditions.

Values are shown as mean ± SEM. (++,+++) indicate significant increase, (#) significant decrease compared to the respective genotype without the drug. Statistical evaluation was performed using one way ANOVA with application of post hoc Tukey's test for multiple comparisons. See supplementary tables 1–3 for details on the statistics. P, days post natal; DIV, days *in vitro;* mush., mushroom-shaped spine. *$p<0.05$, (++)(##)$p<0.01$, ***(+++)$p<0.001$. Scale bar: 5 μm.

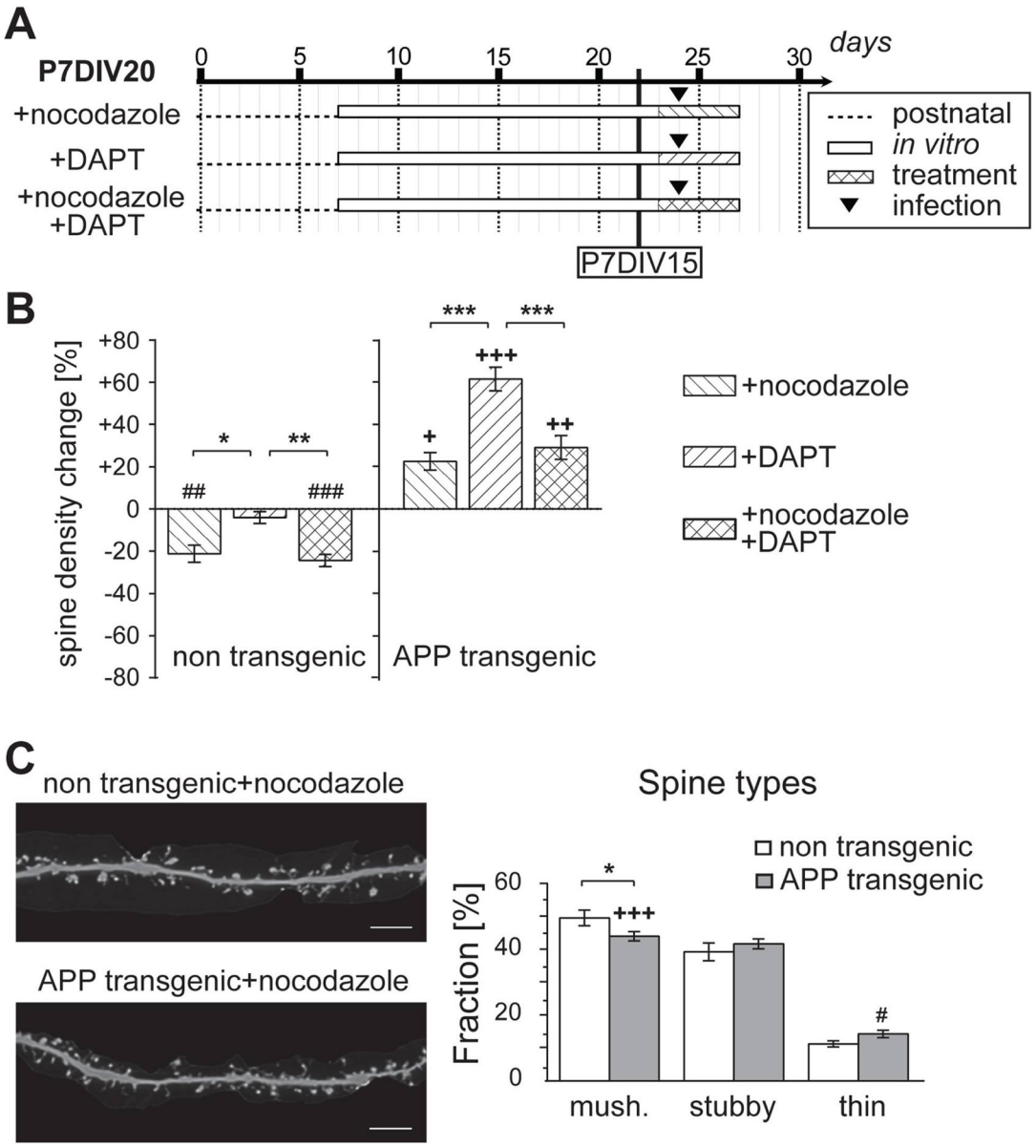

Figure 4. Effect of nocodazole on spine density and DAPT-induced reversal of spines

A. Schematic representation showing the experimental set-up to analyze the effect of nocodazole alone and on DAPT-induced spine recovery. Conditions, where spine changes were already evident in cultures from APP_{SDL} transgenic mice (P7DIV15), are indicated. **B**. Effect of nocodazole, DAPT, and the combination of both drugs in APP_{SDL} transgenic and non-transgenic cultures in CA1 neurons. Spine density changes compared to the respective experiments without drug (non-transgenic and APP_{SDL} transgenic cultures, respectively) are shown right. Nocodazole suppresses DAPT-induced spine reversal in APP_{SDL} transgenic cultures. **C**. Effect of nocodazole-treatment on spine shape in CA1 neurons. Representative high-resolution images of dendritic segments after treatment with nocodazole are shown on the left. Differences compared to the respective genotype without the drug are indicated.

Nocodazole changes the spine population from APP_{SDL} transgenic mice towards an increased fraction of mushroom spines.

Values are shown as mean ± SEM. (+,++,+++) indicates significant increase, (#,##,###) significant decrease compared to the respective genotype without the drug. Statistical evaluation was performed using one way ANOVA with application of post hoc Tukey's test for multiple comparisons. See supplementary tables 1 and 3 for details on the statistics. *(+)(#)$p<0.05$, **(++)(##)$p<0.01$, ***(+++)(###)$p<0.001$. P, days post natal; DIV, days *in vitro;* mush., mushroom-shaped spine. Scale bar: 5μm.

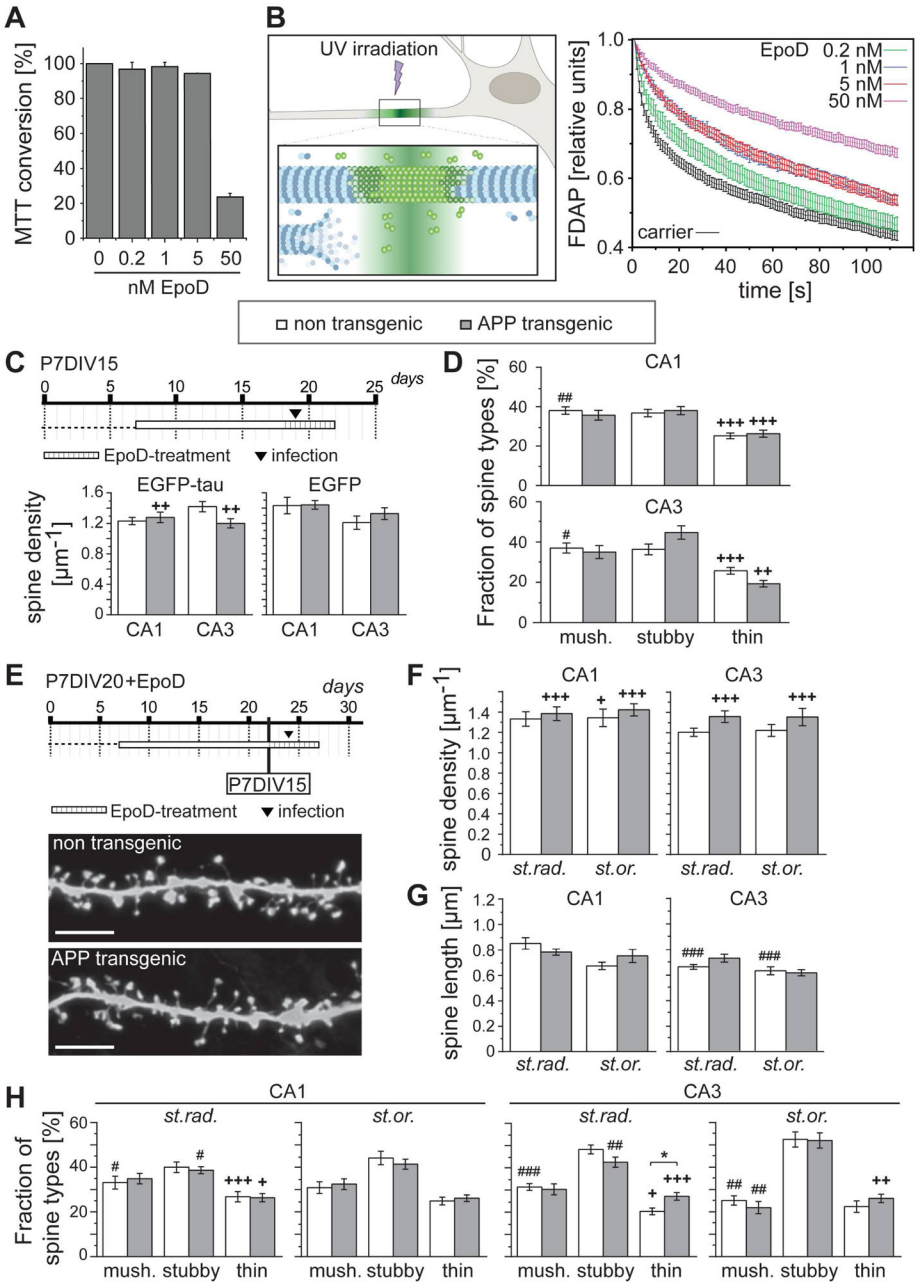

Figure 5. Effect of Epothilone D on cell survival, MT polymerization and spine density and morphology

A. Effect of EpoD on the survival of PC12 cells as determined by MTT conversion. The carrier control (0.01% DMSO) is set as 100%. **B**. Measurement of FDAP to determine MT dynamics in neuronal processes. Neuronally differentiated PC12 cells expressing PAGFP-tagged tubulin were focally irradiated with an UV laser in the middle of a process. FDAP, as an indicator for the ratio of soluble to polymerized tubulin, was determined in the region of activation. The respective FDAP plots of cells treated with carrier (0.01% DMSO), and different concentrations of EpoD are shown to the right. EpoD induces a decreased FDAP indicative for MT stabilization, which is evident already at 0.2 nM. Note that the curves for

1 and 5 nM EpoD (blue and red, respectively) run together very close. **C**. Schematic representation showing the experimental set-up to analyze the effect of EpoD in short term cultures (P7DIV15). Effect of EpoD treatment on spine density after expression of EGFP-tau or EGFP alone in CA1 and CA3 neurons are shown at the bottom. EpoD abolishes the difference between Aβ-producing and control cultures by increasing the spine density in APP transgenic cultures. No difference due to the expressed construct (EGFP-tau or EGFP) is observed. **D**. Effect of EpoD-treatment on spine shape in CA1 and CA3 neurons after expression of EGFP-tau. Differences compared to the respective genotype without the drug are indicated. EpoD changes the spine population from APP_{SDL} transgenic and non transgenic mice towards an increased fraction of thin spines. **E**. Schematic representation showing the experimental set-up to analyze the effect of EpoD on spine recovery. Conditions, where spine changes were already evident in cultures from APP_{SDL} transgenic mice (P7DIV15), are indicated. Representative high-resolution images of dendritic segments after treatment with EpoD are shown at the bottom. **F–G**. Effect of EpoD-treatment on spine densities (F), spine lengths (G), and spine shape (H) in CA1 and CA3 neurons. Differences compared to the respective genotype without the drug are indicated. EpoD abolishes the difference between Aβ-producing and control cultures with respect to all parameters. Note that EpoD induces an increase in the fraction of thin spines, which is evident at most conditions.

In (A), mean and range from two independent experiments with three technical replicates each are shown. FDAP curves in B are based on n = 11–24 measurements per experimental condition. In (C–H), values are shown as mean ± SEM. (+,++,+++) indicate significant increase, (#,##,###) significant decrease compared to the respective genotype without the drug. Statistical evaluation was performed using one way ANOVA with application of post hoc Tukeys's test for multiple comparisons. See supplementary tables 1–3 for details on the statistics. *(+)(#)$p<0.05$, (++)(##)$p<0.01$, (+++)(###)$p<0.001$. *st.or.*, *stratum oriens; st.rad.*, *stratum radiatum*; P, days post natal; DIV, days *in vitro;* mush., mushroom-shaped spine. Scale bar: 5 μm.